Korean Chem. Eng. Res., 55(5), 698-703 (2017)
https://doi.org/10.9713/kcer.2017.55.5.698
PISSN 0304-128X, EISSN 2233-9558

Two- and Three-dimensional Analysis on the Bubble Flow Characteristics Using CPFD Simulation

Jong Hun Lim and Dong Hyun Lee†

School of Chemical Engineering, Sungkyunkwan University, 2066, Seobu-ro, Jangan-gu, Suwon, 16419, Korea

(Received 26 March 2017; Received in revised form 17 May 2017; accepted 1 July 2017)

Abstract – Bubble flow characteristics in fluidized beds were analyzed by CPFD simulation. A fluidized bed, which had the size of 0.3 m-ID × 2.4 m-high, was modeled by commercial CPFD Barracuda®. Properties of bed material were $d_p = 150$ μm, $\rho_p = 2{,}330$ kg/m^3, and $U_{mf} = 0.02$ m/s. Gas was uniformly distributed and the range of superficial gas velocity was 0.07 to 0.16 m/s. Two other geometries were modeled. The first was a three-dimensional model, and the other was a two-dimensional model of 0.01 m × 0.3 m × 2.4 m. Bubble size and rising velocity were simulated by axial and radial position according to superficial gas velocity. In the case of three-dimensional model, simulated bubble rising velocity was different from correlations, because there was zigzag motion in bubble flow, and bubble detection was duplicated. To exclude zigzag motion of bubble flow, bubble rising velocity was simulated in the two-dimensional model and compared to the result from three-dimensional model.

Key words: Fluidized beds, CPFD simulation, Bubble flow characteristics

1. Introduction

Bubbling fluidized beds are a typical fluidized beds that have been widely used in the chemical industry. During this process, fluidized reactors are operated under bubbling fluidized conditions, and the gas bubbles formed by the excess exertion of gas can affect the residence time of the gas and particles, heat and mass transfer, particle entrainment, and reaction conversion. There are experimental techniques for measuring of bubble size and rising velocity, such as probe, image photographing, and radiograph [1] However, experimental measurement of bubble flow is not possible in all cases. Therefore, many researchers have investigated bubble flow characteristics using computational fluid dynamics (CFD), not directly experimentation. Moreover, recently, computational particle-fluid dynamics (CPFD) has been used in analysis of bubble flow characteristics in fluidized beds. There is research of bubble flow characteristics using CPFD.

To investigate bubble flow characteristics in fluidized beds, bubble rising velocity was simulated by CPFD simulation. Bubble rising velocity was calculated according to axial height and radial position by transient data of particle volume fraction that was obtained from simulation with two- and three-dimensional models. Simulated bubble rising velocity was compared to correlations for bubble rising velocity.

†To whom correspondence should be addressed.
E-mail: dhlee@skku.edu
‡This article is dedicated to Prof. Jea Keun Lee on the occasion of his retirement from Pukyong National University.

2. Theoretical Background

2-1. Governing equations of CPFD simulation

Barracuda uses a multiphase particle-in-cell (MP-PIC) approach to calculate the particle–fluid dynamics through the Eulerian-Lagrangian approach. Eulerian approach is applied to gas phase, and Lagrangian approach is applied to particle phase. MP-PIC model uses the concept of computational particle, which is the representative particle in each size distribution decided by probability distribution. More detailed descriptions and governing equations are listed in Snider's research [2].

2-2. Correlations of bubble properties

Karimipour and Pugsley [1] investigated many correlations for bubble size and bubble rising velocity, and suggested a suitable correlation for each Geldart group. There are correlations for Geldart group B particles as follows: Cai *et al.* [3] or Mori and Wen [4] for bubble size, and Davidson and Harrison [5] for bubble rising velocity.

2-2-1. Initial bubble size

A few correlations of the initial bubble size for porous distributors have been proposed. The correlations of Miwa *et al.* [6] that have been used by the majority of researchers are as follows:

$$d_0 = 0.00376(U_o - U_{mf})^2 \tag{1}$$

2-2-2. Bubble size in the bed

Empirical correlations about bubble diameter with a bed height suitable for this study are shown by the following equations:

Cai *et al.* [3]

$$d_b = 0.138h^{0.8}(U_o - U_{mf})^{0.42} \exp(-2.5\times10^{-5}(U_o - U_{mf})^2 - 10^{-3}(U_o - U_{mf})) \tag{2}$$

Mori and Wen [4]

$$\frac{d_{bm}-d_b}{d_{bm}-d_0} = \exp(-0.3h/D) \quad (3)$$

$$d_{bm} = 0.652[A(U_o-U_{mf})]^{2/5} \quad (4)$$

2-2-3. Bubble rising velocity in the bed

Bubble rising velocity was predicted by above empirical correlations about bubble diameter by the correlation of Davidson and Harrison [5]:

$$U_{br} = 0.71\sqrt{gd_b} \quad (5)$$

$$U_b = U_{br}+(U_o-U_{mf}) \quad (6)$$

3. Simulation Setup

Fig. 1 shows the portion of three-dimensional geometry model of the fluidized beds used in the simulation. Metal-grade silicon (MG-Si) particles weighing 75 kg were placed in a column of dimensions 0.3 m ID × 2.4 m high [7,8]. Static bed height was 0.8 m. Material properties and particle size distribution of bed material are shown in Table 1 and Fig. 2. Bed material is categorized in Geldart group B.

Total number of cells in the three-dimensional model was 192,000. Inlet boundary condition was set to uniform gas distribution. Superficial gas velocities were 0.07, 0.1, 0.13, and 0.16 m/s. Model and parameters are the same as listed in Lim *et al*. [9]. Boundary conditions are listed in Table 2.

Fig. 3 shows the criterion of the classification of bubble and emulsion phase. In this figure, the particle volume fraction, which is criterion of classification of bubble and emulsion, can be found. From these results, a criterion of classification of bubble was decided as 0.43 of particle volume fraction.

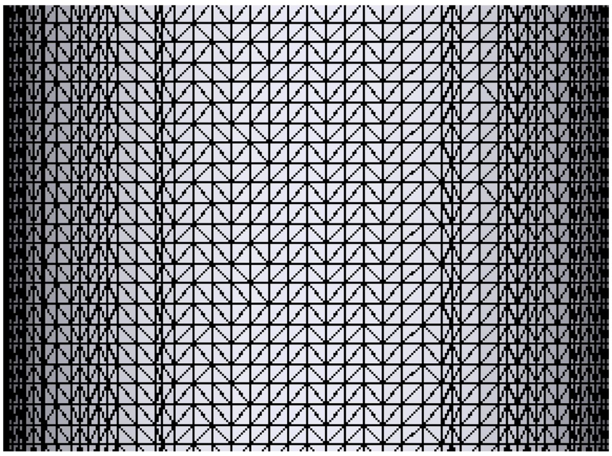

Fig. 1. The portion of three-dimensional geometry model of the fluidized beds.

Table 1. Material properties of bed material

Mean diameter (μm)	149
Particle density (kg/m^3)	2325
Bulk density (kg/m^3)	1180
Sphericity (-)	0.75
Minimum Fluidization Velocity (m/s)	0.02

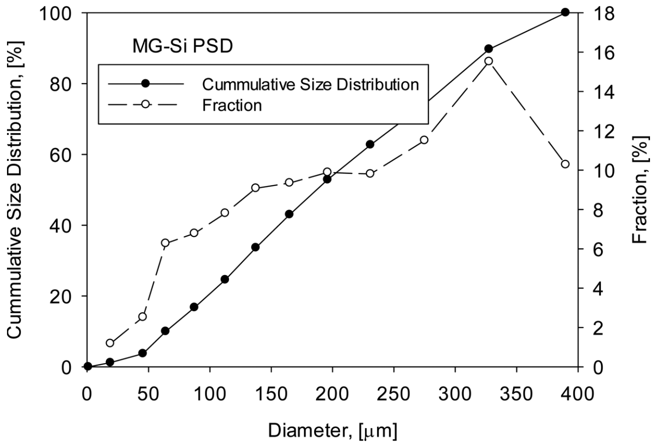

Fig. 2. Particle size distribution of bed material.

Table 2. Boundary conditions for the simulation

Diameter (3D model)	0.3 m
Width (2D model)	0.3 m
Thickness (Only 2D model)	0.01 m
Initial bed height	0.8 m
Total weight of bed inventory (Only 3D model)	75 kg
Range of U_o	0.07 to 0.16 m/s
Temperature	300 K
Pressure	101325 Pa
Fluidizing gas	Air
Simulation time	60 s

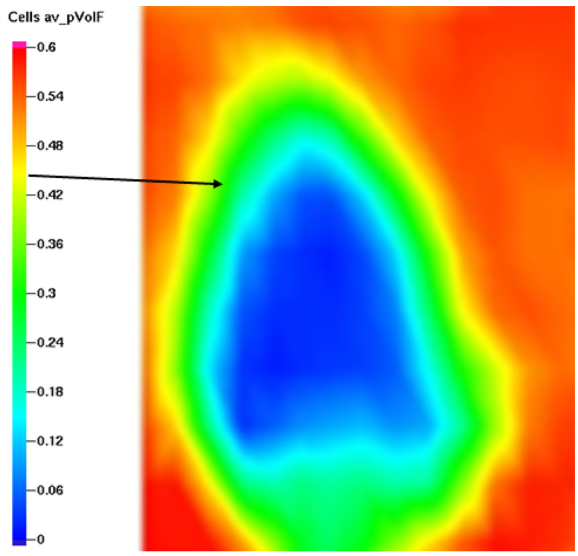

Fig. 3. Snapshot of a bubble.

Fig. 4(a) shows bubble rising according to time with axial cross–sectional view. Fig. 4(b) shows a schematic diagram of the calculation of bubble rising velocity from particle volume fraction by moving distance of bubble and time difference, which are shown in Fig. 4(a). Fig. 4(c) shows the transient data which are sampled in two different data sampling positions [10]. When bubble is passed through data sampling position, particle volume fraction is decreased under criterion of

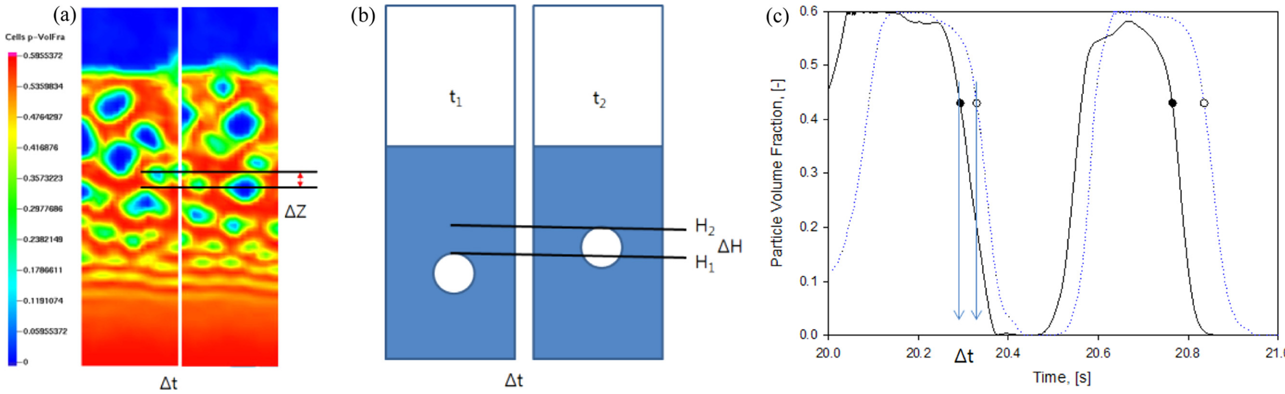

Fig. 4. (a) Description for determination of bubble rising velocity from simulation data (b) schematic diagram of bubble rising velocity (c) description of calculation of bubble rising velocity from particle volume fraction data.

classification of bubble phase. In this timing, it is recognized that the top of bubble passes through a sampling point. Bubble rising velocity could be calculated by distance of two sampling positions and time difference from particle volume fraction data:

$$U_b = \Delta H/\Delta t \tag{7}$$

Axial heights of transient sampling positions were 0.4 and 0.7 m in each superficial gas velocity. Radial positions were r/R=0.03, 0.21, 0.40, 0.65 and 0.85. Simulation time was 30 s in each case. Bubble rising velocity was calculated from average of transient data in 20~30 s. The distance between upper point and bottom point was 0.02 m. To compare between two-, and three-dimensional models, the two-dimensional fluidized bed was simulated, which had the same height and width of three-dimensional model in the same operating conditions.

4. Results and Discussion

4-1. Three-dimensional model analysis

Fig. 5 shows the cross–sectional view of beds at U_o = 0.1 m/s, and H = 0.7 m. This figure shows the relationship between single bubble and data sampling positions. As shown, a bubble occupied two or more data sampling positions. Therefore, one bubble was duplicated to many bubbles. In Fig. 4(a), bubble size and radial position was varied according to rising of velocity. This effect of bubble rising velocity was calculated by transient data from two sampling positions. Therefore, bubble rising velocity of single bubble may be different according to data sampling position.

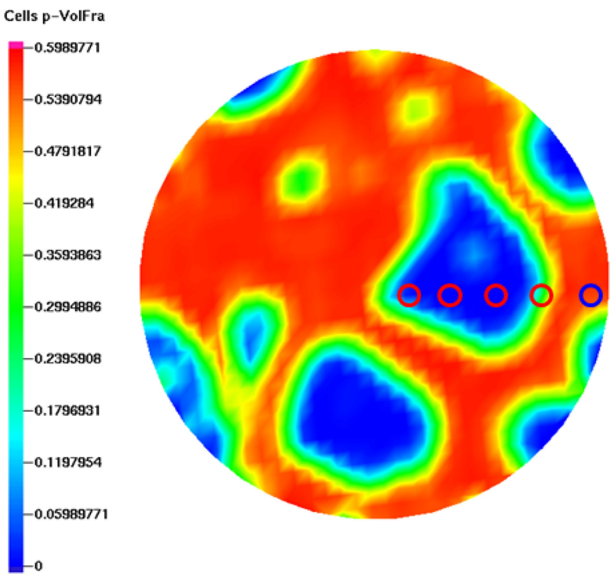

Fig. 5. Duplication of single bubble in radial cross-ectional view (U_o = 0.1 m/s, Z = 0.7 m).

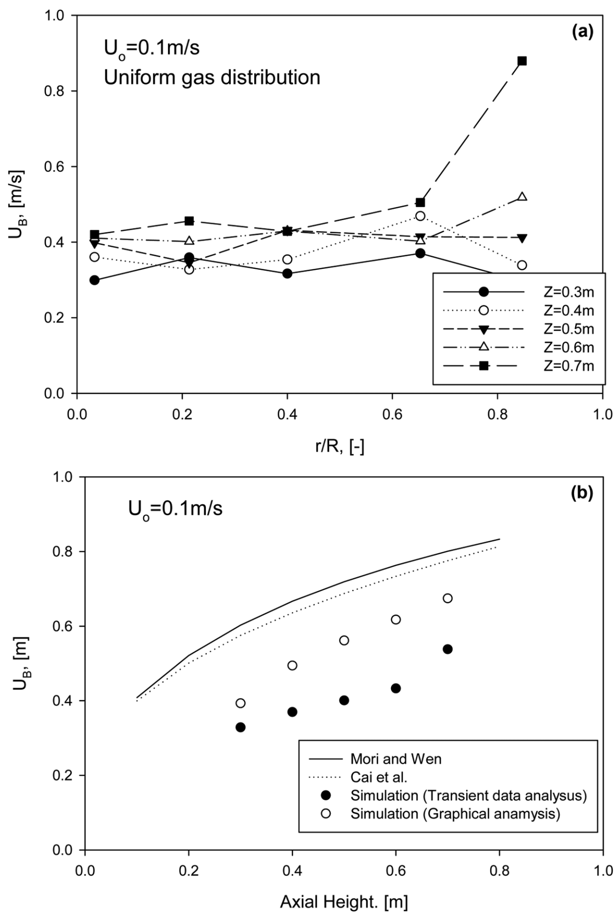

Fig. 6. (a) Average bubble rising velocity according to radial position, (b) Comparing between simulation and correlations for average bubble rising velocity.

Fig. 6 shows the average of bubble rising velocity by transient data at $U_o = 0.1$ m/s according to radial position and axial height. In Fig. 6(a), There was no significant tendency in bubble rising velocity according to radial position at lower height. At Z = 0.7, bubble rising velocity at r/R = 0.21 (center) and r/R = 0.85 (near the wall) was higher than other radial position. This was because most of the bubbles passed through the center of bed and some of the bubbles were near the wall. Fig. 6(b) shows the comparing between simulation and correlations for average bubble rising velocity. Bubble rising velocity was increased according to axial height. Average bubble rising velocity by transient data was slower than Cai *et al*. [3], or Mori and Wen [4]. Simulation data was lower than correlations that differ from 40%. Also, bubble rising velocity by transient data was lower than graphical analysis using snapshots. Bubble rising velocity calculated by graphical analysis was slower than correlations which differed from 21%, because bubble rising velocities of all individual bubble were averaged without filtering of duplicated bubble in spite of duplication of single bubble, as shown in Fig. 5 This result shows that average bubble rising velocity from transient data without filtering could not explain bubble flow characteristics.

Fig. 7 shows bubble rising velocity at axial height of 0.4 m and 0.7 m in each superficial gas velocity. Fig. 7(a) shows bubble rising velocity according to radial position in the axial height of 0.4 m, and Fig. 7(b) shows in 0.7 m. Bubble rising velocity was significantly increased according to superficial gas velocity at Z = 0.7 m. However, difference of bubble rising velocity at Z = 0.4 m was insignificant according to U_o from 0.07 to 0.13 m/s. Fig. 7(c) and (d) shows average bubble rising velocity according to axial height. Simulated bubble rising velocity was compared to correlations. In lower height (Z = 0.4 m), average bubble rising velocity by transient data was more different from correlation.

Fig. 8 shows the frequency distribution of all individual bubble rising velocities at axial height of 0.7 m, and compared to average bubble rising velocity or correlations. As shown in the figures, bubble rising velocity by transient data has wide distribution. Bubble rising velocity calculated by correlation was located between mean velocity and maximum velocity. At $U_o = 0.07$ m/s, bubble rising velocity calculated by correlations was located in 91% of cumulative bubble rising velocity in frequency distribution. At $U_o = 0.1$ m, 0.13, 0.16 m/s, bubble rising velocity was located at 87%, 83%, and 73%, respectively.

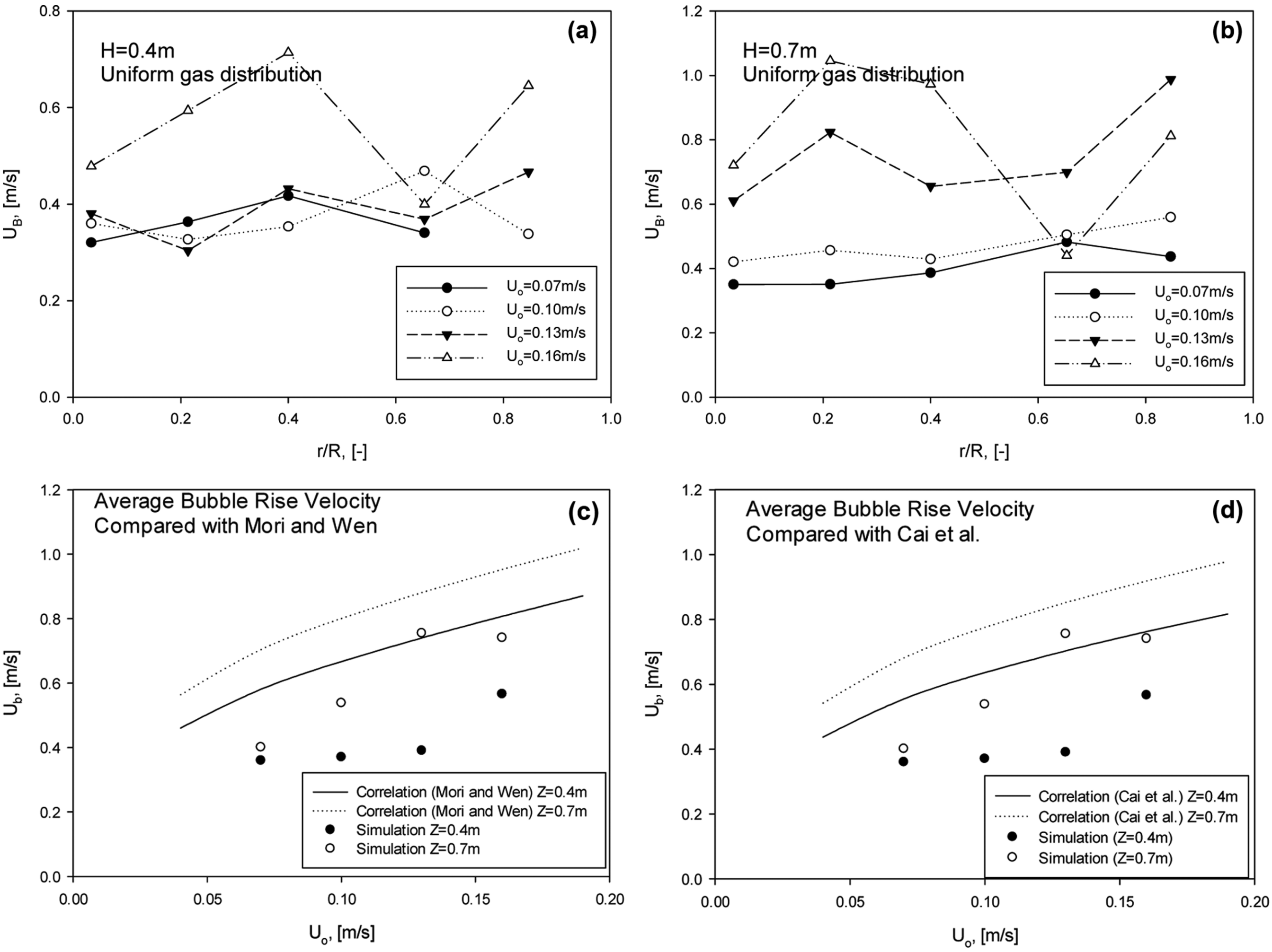

Fig. 7. (a~b) Bubble rising velocity according to radial position, (c~d) Bubble rising velocity according to superficial gas velocity.

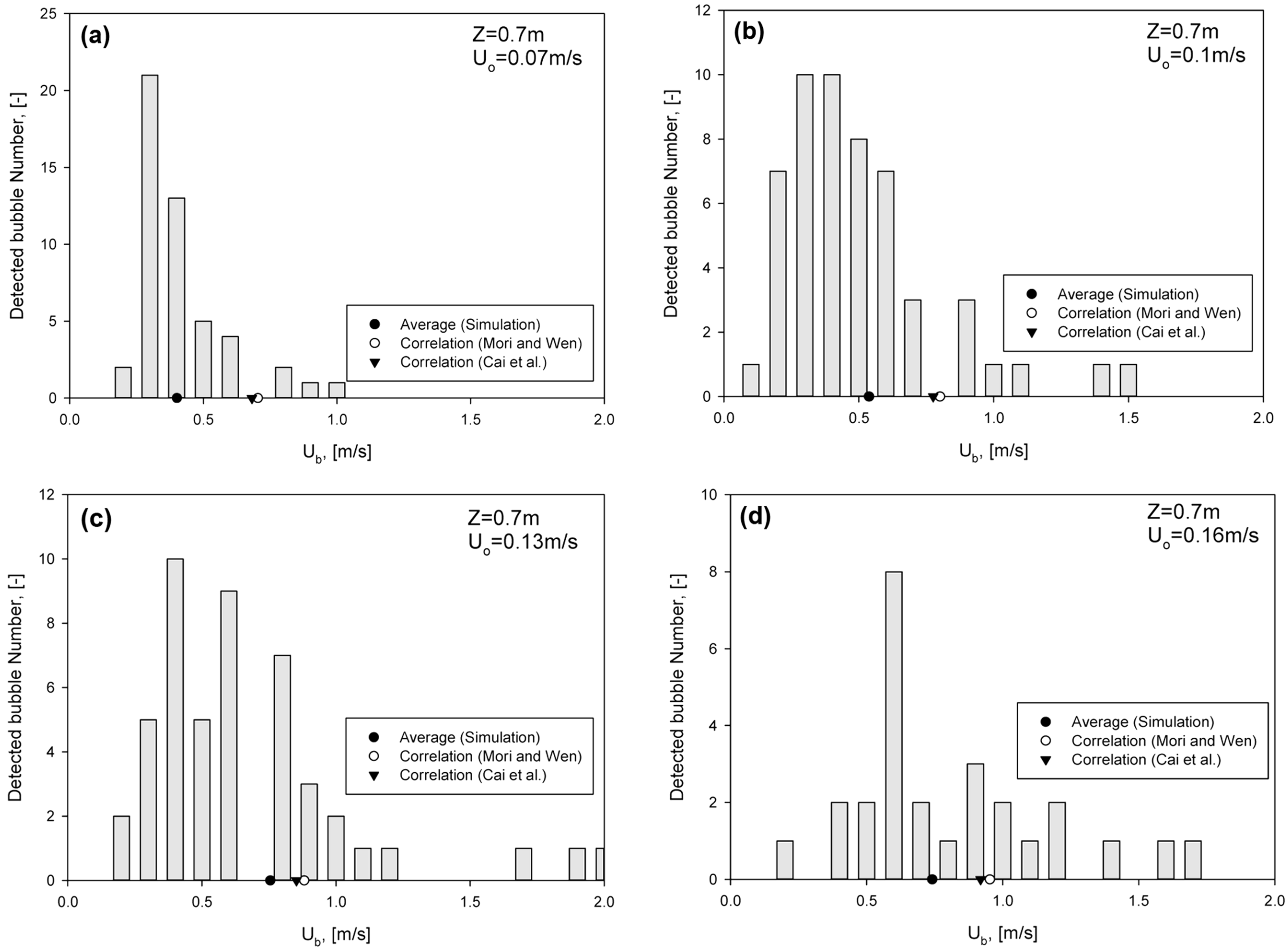

Fig. 8. Distribution of measured bubble rising velocity of all individual bubbles, (a) U_o = 0.07 m/s, (b) U_o = 0.1 m/s, (c) U_o = 0.13 m/s, (d) U_o = 0.16 m/s.

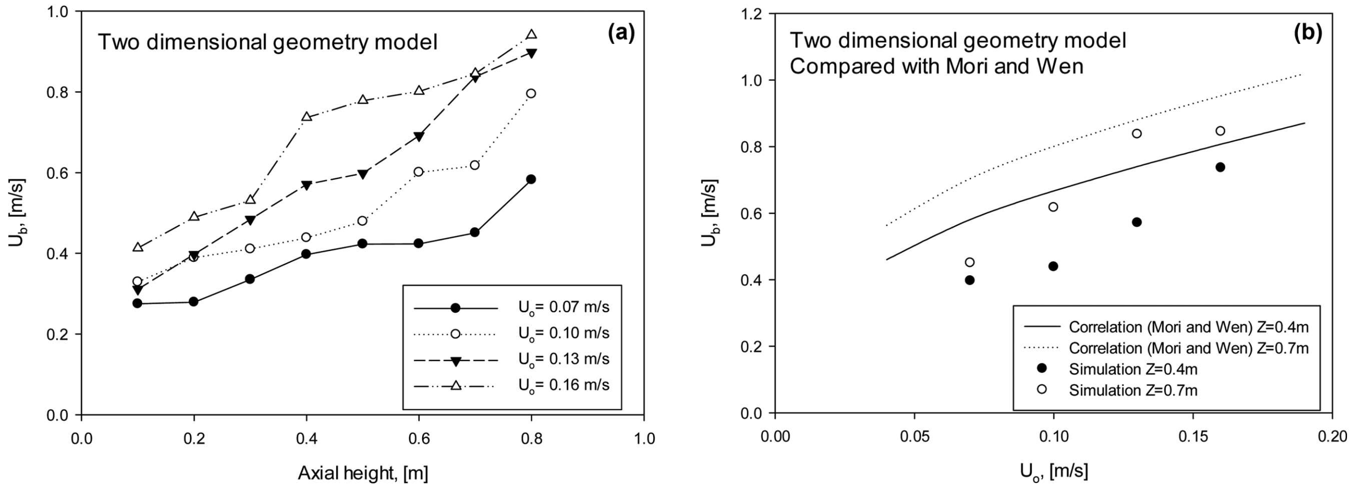

Fig. 9. Result of two-dimensional simulation (a) Bubble rising velocity according to radial position, (b) Comparing between simulation and correlation of Mori and Wen [4].

4-2. Two-dimensional model analysis

Fig. 9 shows the results of two-dimensional simulation. Compared with Fig. 6(b) and Fig. 7(c), simulated bubble rising velocity was slower than correlations still. However, the tendency of simulation results was more proportional to axial height or superficial gas velocity than 3D simulation results. And bubble rising velocity was closer to the correlation of Mori and Wen [4] than 3D simulation results. This result was caused by excluding zigzag motion of bubbles in the bed by replacement from 3D model to 2D model. For accurate analysis, irregular movement of bubble should be avoided as much as possible. Therefore, it could be considered that two-dimensional analysis on the bubble flow is more appropriate than three-dimensional analysis.

5. Conclusions

Bubble rising velocity by transient data differed to graphical analysis due to duplicated bubble detection. Therefore, bubble rising velocity by transient data was slower than by graphical analysis. Also, simulated bubble rising velocity was slower than correlation of Cai *et al*. [3] or Mori and Wen [4]. In the 3D model simulation, Bubble rising velocity was proportional to superficial gas velocity. In lower superficial gas velocity (U_o = 0.07, 0.1 m/s), bubble rising velocity by transient data was more different from correlations than higher gas velocity (U_o = 0.13, 0.16 m/s). In bubble rising velocity distribution, bubble rising velocity by correlation was located at intermediate between average and maximum bubble rising velocity by simulation. In the 2D simulation, simulation result was more proportional to gas velocity and height. And results were closer than 3D simulation.

The simulation model is a preliminary step for designing and conducting actual experiment tests. Therefore, additional experiments are required to validate the simulation result. However, analyses on the bubble flow by insertions such as optical probe, pressure transducer are affected by bubble chord length, and motion of bubbles.

Acknowledgment

This work was supported by the Korea Institute of Energy Technology Evaluation and Planning (KETEP) grant funded by the Korea government Ministry of Trade, Industry and Energy (No. 20163010050070). This work was also supported by the Technology Innovation Program (10052751) funded by the Ministry of Trade, Industry & Energy (MOTIE, Korea).

Nomenclature

A : Bed cross-sectional area [m^2]
D : Bed diameter [m]
d_b : Bubble diameter [m]
d_{bm} : Maximum bubble diameter [m]
d_o : Orifice diameter [m]
d_p : Mean particle diameter [μm]
g : gravitational acceleration [m/s^2]
ΔH : Distance of two sampling positions [m]
r : Radial position of measurement in the radial cross-section of beds [m]
R : Radius of bed column [m]
Δt : Time difference [s]
U_b : Bubble rising velocity [m/s]
U_{br} : Relative bubble rising velocity [m/s]
U_{mf} : Minimum fluidizing velocity [m/s]
U_o : Superficial gas velocity [m/s]
Z : Axial height [m]
ρ_p : Particle density [kg/m^3]

References

1. Karimipour, S. and Pugsley, T., "A Critical Evaluation of Literature Correlations for Predicting Bubble Size and Velocity in Gas-solid Fluidized Beds," *Powder Technology*, **205**(1), 1-14(2011).
2. Snider, D. M., "An Incompressible Three-Dimensional Multiphase Particle-in-Cell Model for Dense Particle Flows," *J. of Computational Physics*, **170**(2), 523-549(2001).
3. Cai, P., Schiavetti, M., Michele, G. D. and Grazzini, G. C., "Quantitative Estimation of Bubble Size in PFBC," *Powder Technology*, **80**(2), 99-109(1994).
4. Mori, S. and Wen, C.Y., "Estimation of Bubble Diameter in Gaseous Fluidized Beds," *AIChE J.*, **21**(1), 109-115(1975).
5. Davidson J. F. and Harrison, D., *Fluidized particles*, Cambridge University Press, London (1963).
6. Miwa, K., Mori, S., Kato, T. and Muchi, I., "Behavior of Bubbles in Gaseous Fluidized Bed," *Int. Chem. Eng.*, **12**, 187-194(1972).
7. Lim, J. H., Lee, Y., Shin, J. H., Bae, K., Han, J. H. and Lee, D. H., "Hydrodynamic Characteristics of Gas-solid Fluidized Beds with Shroud Nozzle Distributors for Hydrochlorination of Metallurgical-grade Silicon," *Powder Technology*, **266**, 312-320(2014).
8. Lim, J. H., Shin, J. H., Bae, K., Kim, J. H., Lee, D. H., Han, J. H. and Lee, D. H., "Hydrodynamic Characteristics of Bubbles in Bubbling Fluidized Bed with Internals," *Korean J. of Chem. Eng.*, **32**(9), 1938-1944(2015).
9. Lim, J. H., Bae, K., Shin, J. H., Kim, J. H., Lee, D. H., Han, J. H. and Lee, D. H., "Effect of Particle-Particle Interaction on the Bed Pressure Drop and Bubble Flow by Computational Particle-Fluid Dynamics Simulation of Bubbling Fluidized Beds with Shroud Nozzle," *Powder Technology*, **288**, 315-323(2016).
10. Lim, J. H., Bae, K., Shin, J. H., Lee, D. H., Han, J. H. and Lee, D. H., "CPFD Simulation of Bubble Flow in a Bubbling Fluidized Bed with Shroud Nozzle Distributor and Vertical Internal," *Korean Chemical Engineering Research*, **54**(5), 678-686(2016).